Tunable molecular orientation and elevated thermal stability of vapor-deposited organic semiconductors

Shakeel S. Dalal[a,1], Diane M. Walters[a,1], Ivan Lyubimov[b], Juan J. de Pablo[b], and M. D. Ediger[a,2]

[a]Department of Chemistry, University of Wisconsin–Madison, Madison, WI 53706; and [b]Institute for Molecular Engineering, University of Chicago, Chicago, IL 60637

Edited by Frank H. Stillinger, Princeton University, Princeton, NJ, and approved February 27, 2015 (received for review November 3, 2014)

Physical vapor deposition is commonly used to prepare organic glasses that serve as the active layers in light-emitting diodes, photovoltaics, and other devices. Recent work has shown that orienting the molecules in such organic semiconductors can significantly enhance device performance. We apply a high-throughput characterization scheme to investigate the effect of the substrate temperature ($T_{substrate}$) on glasses of three organic molecules used as semiconductors. The optical and material properties are evaluated with spectroscopic ellipsometry. We find that molecular orientation in these glasses is continuously tunable and controlled by $T_{substrate}/T_g$, where T_g is the glass transition temperature. All three molecules can produce highly anisotropic glasses; the dependence of molecular orientation upon substrate temperature is remarkably similar and nearly independent of molecular length. All three compounds form "stable glasses" with high density and thermal stability, and have properties similar to stable glasses prepared from model glass formers. Simulations reproduce the experimental trends and explain molecular orientation in the deposited glasses in terms of the surface properties of the equilibrium liquid. By showing that organic semiconductors form stable glasses, these results provide an avenue for systematic performance optimization of active layers in organic electronics.

glasses | organic semiconductors | molecular orientation | physical vapor deposition | high-throughput characterization

Glasses (or amorphous solids) of low molecular weight organic compounds exhibit desirable properties for organic electronics. Because these materials are made from organic molecules, properties that depend on chemical identity such as optical absorptions, bandgap, and glass transition temperature can be tuned via chemical synthesis. These glasses have solid-like mechanical properties similar to those of crystalline materials, but offer morphological homogeneity, greater ease of processing, and nearly unlimited compositional tunability. An underappreciated feature of these materials, a result of their nonequilibrium nature, is that many different glasses can be prepared with the same chemical composition.

There has been considerable recent interest in controlling molecular orientation in organic semiconducting glasses (1–7). Whereas one might expect all glasses to be isotropic because of their structural disorder, Yokoyama et al. and other groups have shown that molecular orientation in vapor-deposited glasses can be quite anisotropic (3, 4, 8, 9) and depend upon deposition conditions (3). It has recently been suggested that orientation resulting from deposition could be used as a figure of merit to identify promising compounds for these applications (10). Oriented materials can increase light outcoupling by a factor of 1.5 by directing emission out of the plane of the device (10–14). It has also been shown that oriented layers can improve device lifetime (15) and charge mobility (16–18). Given the potential utility of controlling molecular orientation in device layers (4, 5, 7), it is desirable to understand the extent to which molecular orientation can be tuned in glasses made from a particular compound and the mechanistic origins of this effect. Anisotropic glassy solids are also of interest for applications in optics and optoelectronics (19).

Concurrently, other investigators have shown that vapor-deposited glasses can have desirable physical properties unobtainable by any other means, when the substrate temperature during deposition ($T_{substrate}$) is held somewhat below the glass transition temperature (T_g). Discovered using model glass formers and labeled "stable glasses," these glasses have lower enthalpies (20), higher densities (21), and resist structural reorganization to higher temperatures than is possible with any other preparation route (22–24). The properties of stable glasses are explained by the high mobility of the free surface during the vapor deposition process (20, 25). Because of lowered constraints to motion (26), molecules near the free surface can adopt near-equilibrium packing arrangements during deposition even at temperatures where the bulk structural relaxation time is thousands of years (21, 27). Subsequent deposition traps this efficient packing into the bulk solid. Like organic semiconductors, stable glasses can be birefringent (21) and also anisotropic in wide-angle X-ray scattering (28, 29).

Here we show that organic semiconductors form stable glasses, and that surface mobility during vapor deposition governs bulk molecular orientation in these materials. Using a high-throughput experimental scheme, we are able to efficiently characterize the effect of $T_{substrate}$ on three organic compounds used in semiconducting devices: TPD, NPB, and DSA-Ph [Fig. 1*E*; N,N'-Bis(3-methylphenyl)-N,N'-diphenylbenzidine, N,N'-Di(1-napthyl)-N,N'-diphenyl-(1,1'-biphenyl)-4,4'-diamine, and 1–4-Di-[4-(N,*N*-diphenyl)amino]styryl-benzene, respectively]. We find that these

Significance

Glasses are solids that lack the regular order of crystals. Organic glasses, when produced by deposition from the vapor, can exhibit high levels of molecular orientation that improve performance of devices such as organic light-emitting diodes. We show here that molecular orientation in such glasses is primarily controlled by the substrate temperature during deposition, suggesting that the performance of almost any device based upon amorphous organic materials might be systematically optimized by this route. We explain molecular orientation in the glass in terms of the orientation present near the surface of the corresponding liquid. The highly oriented glasses formed here also exhibit high density and improved thermal stability. These features will likely further enhance the performance of organic electronics devices.

Author contributions: S.S.D., I.L., J.J.d.P., and M.D.E. designed research; S.S.D., D.M.W., and I.L. performed research; S.S.D., D.M.W., I.L., J.J.d.P., and M.D.E. analyzed data; and S.S.D. and M.D.E. wrote the paper.

The authors declare no conflict of interest.

This article is a PNAS Direct Submission.

[1]S.S.D. and D.M.W. contributed equally to this work.

[2]To whom correspondence should be addressed. Email: ediger@chem.wisc.edu.

This article contains supporting information online at www.pnas.org/lookup/suppl/doi:10.1073/pnas.1421042112/-/DCSupplemental.

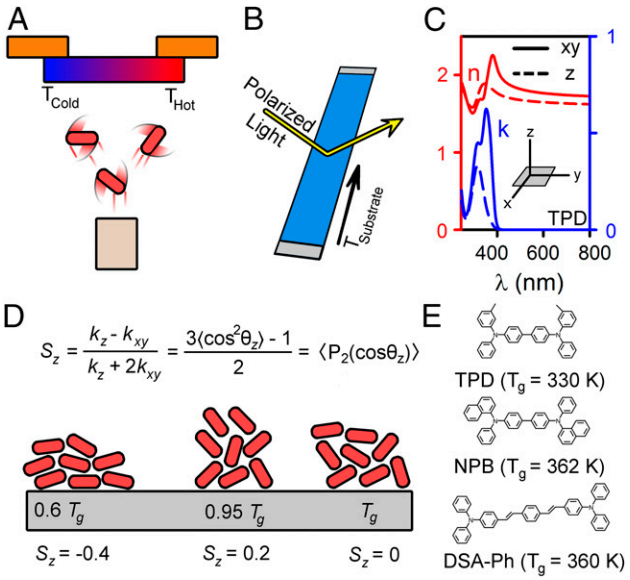

Fig. 1. Schematic illustration of the experimental procedure. (*A*) Organic molecules are vapor-deposited in a vacuum chamber. A silicon substrate with a controlled range of temperatures allows simultaneous deposition of many glasses with different properties but identical chemical composition. (*B*) After vapor deposition, each glass is independently interrogated using spectroscopic ellipsometry with a focused beam. (*C*) Example optical constants for TPD at $T_{substrate}$ = 215 K. The optical constants for light polarized normal to (z) and in the plane of the substrate (xy) can be independently determined (49). (*D*) Using the optical constants, the orientation order parameter, S_z, can be computed at each $T_{substrate}$. θ_z is the angle of the long molecular axis relative to the substrate normal and P_2 is the second Legendre polynomial. (*E*) Structures and glass transition temperatures for the three compounds studied.

compounds form stable glasses, and we show that the orientation of the vapor-deposited molecules is controlled by $T_{substrate}/T_g$ and is nearly independent of the molecular aspect ratio. Using simulations, we show that anisotropic molecular orientation in the glass can be understood in terms of molecular orientation and mobility near the free surface of the equilibrium liquid. By connecting two apparently disparate bodies of work, we develop avenues for research on organic devices and the physics of glasses, and further the development of "designer" anisotropic solids.

Results

Fig. 1 illustrates our experimental procedure. Molecules are vapor-deposited in a vacuum chamber with base pressure near 10^{-7} torr onto a substrate with a controlled gradient of temperatures using a previously described apparatus (21). On a single substrate, this produces many glasses with identical chemical composition but different physical properties (*Materials and Methods*). The different glasses are characterized using spectroscopic ellipsometry with Kramers–Kronig consistent models (3). (*SI Text*, *Ellipsometry Measurements; Model Construction*.)

Fig. 2*A* illustrates the determination of key material properties of a vapor-deposited glass using spectroscopic ellipsometry. When the "as-deposited" glass is initially heated, it expands as a solid while maintaining its as-deposited molecular orientation. At T_{onset}, which is greater than T_g for all of the materials reported here, the glass begins to transform into supercooled liquid (SCL). This results in an abrupt change in the film thickness. After the entire sample has become the SCL, it is cooled at a controlled rate. The thickness decreases linearly until the glass transition temperature, T_g, after which the material falls out of equilibrium and becomes the ordinary, liquid-cooled glass. By comparing the film thickness before and after temperature cycling, we are able to determine the density of the as-deposited glass relative to the ordinary glass ($\Delta\rho$). For temperature gradient samples, T_{onset} is determined for many glasses during a single heating experiment, whereas $\Delta\rho$ is determined by mapping the sample thickness before and after heating (21).

The three semiconducting compounds investigated here (TPD, NPB, and DSA-Ph) all form stable glasses via vapor deposition. This is illustrated in Fig. 2*B* by the high onset temperatures and in Fig. 2*C* by the high densities. The elevated thermal stability of these materials may provide an avenue to increase device lifetime by imparting greater stability to the useful structures formed by

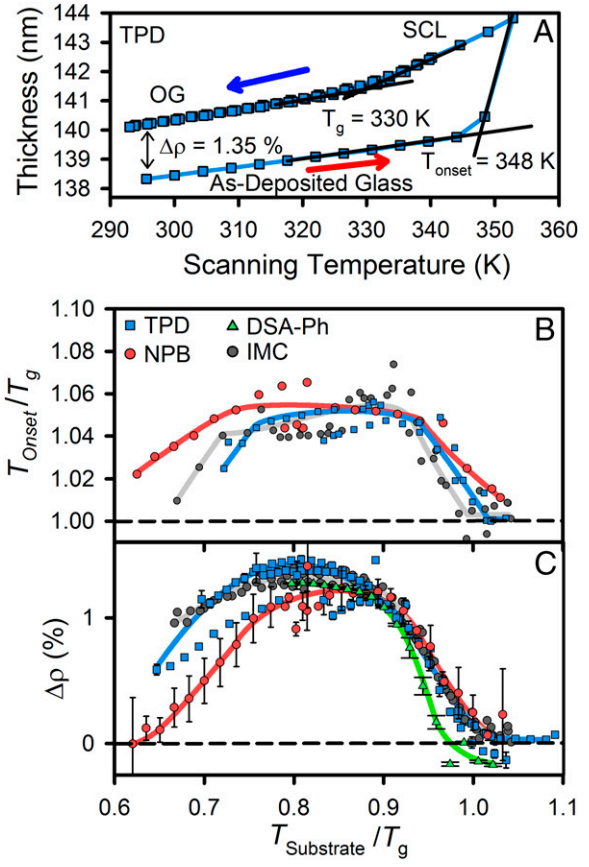

Fig. 2. Properties of as-deposited glasses measured with spectroscopic ellipsometry. (*A*) Sample thickness during heating and cooling for a vapor-deposited glass of TPD ($T_{substrate}$ = 289 K). We compute a relative density, $\Delta\rho$, between the as-deposited glass and the ordinary glass from the change in film thickness. T_{onset}, a measure of structural stability against heating, is the temperature at which the sample begins to transform into the liquid. Each data point represents an independent fit of the optical constants and film thickness at the measurement temperature. (*B*) T_{onset}/T_g for three molecules used as organic semiconductors and one model glass former (21). T_{onset} is greater than T_g for these materials, indicating that more thermal energy is required to dislodge the molecules from their solid-state packing, relative to the liquid-cooled glass. Each data point represents a single, independently characterized material. (*C*) The dependence of $\Delta\rho$ upon $T_{substrate}/T_g$ for glasses made of four compounds. Competition between kinetics and thermodynamics produces materials with many different densities. The T_{onset}/T_g and $\Delta\rho$ data for TPD, NPB, and DSA-Ph are consistent with previous data for IMC (21), a model glass former. The data shown are from 1,064 independently characterized materials (475 are IMC). For only DSA-Ph, $\Delta\rho$ is determined using the Lorentz–Lorenz equation (*SI Text*, *Density Determination for DSA-Ph*) (50–52). Error bars represent 90% confidence intervals (n = 3–6) and are independently calculated for each $T_{substrate}/T_g$ on each sample, and are smaller than the symbol size for most measurements.

vapor deposition (see *Discussion*). The results in Fig. 2 *B* and *C* are in good agreement with previously reported results for indomethacin (IMC) (21), the most extensively studied stable glass former, and can be interpreted as follows. At $T_{substrate}/T_g \geq 1$, surface and bulk mobility are high enough to allow total equilibration at the deposition temperature; when the sample is cooled to 293 K for measurement, it becomes the ordinary glass and has the expected values of T_{onset}/T_g and $\Delta\rho$. At lower values of $T_{substrate}/T_g$, there is a thermodynamic driving force to form the equilibrium SCL at that temperature resulting in higher stability, higher density materials. The mobility of the surface enables molecules to find these tight packing arrangements (20, 25, 27), even though this would require a prohibitively long time for a bulk material. T_{onset}/T_g and $\Delta\rho$ are maximized when high surface mobility is paired with a large thermodynamic driving force. At the lowest $T_{substrate}/T_g$ the surface is so immobile that only marginally stable glasses are formed despite the presence of the largest driving force for densification. Our results are in good agreement with a recent report that NPB forms a stable glass when deposited onto a room-temperature substrate (15).

Using spectroscopic ellipsometry, we find that vapor-deposited glasses of the three compounds are anisotropic, each with continuously tunable average molecular orientation that is well-correlated with $T_{substrate}/T_g$. Fig. 3 shows the order parameter, S_z, and the birefringence as a function of $T_{substrate}/T_g$. Using films

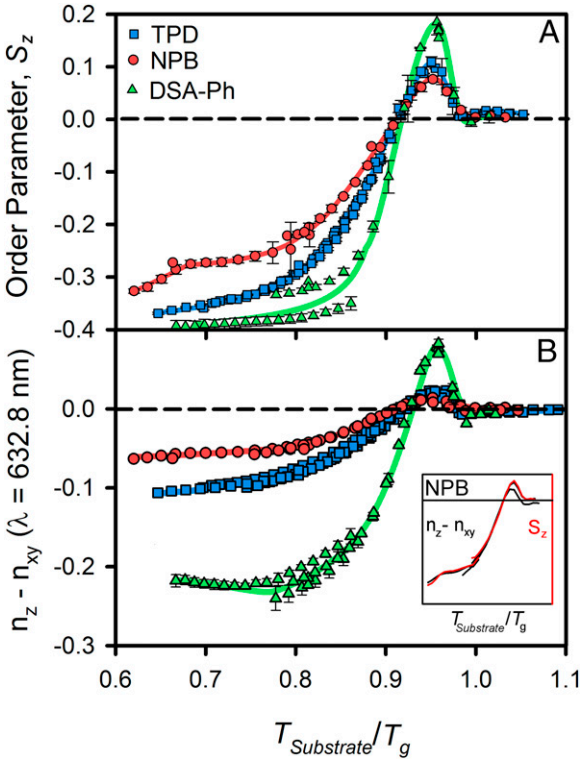

Fig. 3. Measures of molecular orientation as a function of $T_{substrate}/T_g$ for vapor-deposited glasses of three molecules used in organic semiconductors. (*A*) The order parameter S_z reporting the average orientation of molecules in the glass. Fig. 1*D* schematically interprets these results. A wide range of S_z values is accessed and a generic trend is observed for these three linear molecules with different aspect ratios. The data shown are from 612 independently characterized materials. (*B*) The birefringence, which for these materials is also sensitive to the average orientation of the long molecular axis relative to the substrate. The birefringence and S_z show good correspondence, as shown in the inset for NPB. The data shown are from 828 independently characterized materials. Error bars represent 90% confidence intervals (n = 3–6).

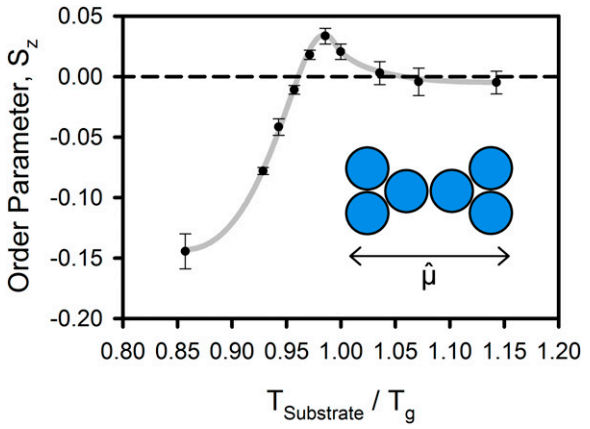

Fig. 4. Order parameter S_z as a function of $T_{substrate}/T_g$ from simulations of vapor-deposited glasses of the inset molecule. These simulations qualitatively reproduce the experimental results shown in Fig. 3*A*. The orientation of the deposited material is defined by comparing the long axis of the molecule to the substrate normal, $S_z = \langle P_2(\hat{\mu}\cdot\hat{z})\rangle$. The T_g obtained by cooling a liquid of these molecules at the lowest accessible rate is 0.70. The error bars represent the standard error of five independently prepared samples.

70–150 nm thick, S_z is computed from the dichroism of the absorption associated with the long axis of each molecule (*SI Text*, *Computing the Orientation Order Parameter*). As shown in Fig. 1*D*, S_z is a measure of the average orientation of the long axis relative to the surface normal. At the lowest temperatures, S_z closely approaches the limit ($S_z = -0.5$) where the long axes of all molecules lie in the plane of the substrate. Such horizontal alignment may be useful in increasing the light outcoupling efficiency of emitting molecules (2), or the absorption of light in the photoactive layer of a solar cell. Using films 70–900 nm thick, the birefringence, $\Delta n = n_z - n_{xy}$, is calculated at 632.8 nm; Δn results from molecular orientation and the anisotropic polarizability tensors of these molecules. By comparing different samples and models, we estimate that the S_z and Δn values reported in Fig. 3 are accurate to $\pm$ 0.05 and $\pm$0.01, respectively.

Our high-throughput methodology allows us to differentiate between the effect of molecular shape and $T_{substrate}/T_g$ for the first time, to our knowledge. The influence of these two variables on molecular orientation has been studied by Yokoyama (3) and our results are broadly consistent with this previous work. Whereas Yokoyama concluded that molecules with more anisotropic shapes produce more anisotropic materials (30, 31), our extended data show in addition that even relatively short molecules like TPD and NPB can be significantly oriented, as long as $T_{substrate}$ is correctly chosen. Given the similar trend observed for the three different compounds studied here, we propose that the parameter which primarily controls the orientation of linear molecules is $T_{substrate}/T_g$ rather than molecular aspect ratio. This is a significant change in perspective, as it suggests that a wide range of molecular orientations might be achieved with almost any organic compound.

To understand the origin of molecular orientation in vapor-deposited glasses, we simulated the vapor deposition of a coarse-grained representation of TPD composed of six Lennard-Jones spheres connected by harmonic springs (Fig. 4, *Inset*). We used a previously described algorithm that mimics the essential features of the deposition process (*Materials and Methods*) (32). A small number of molecules is introduced to the simulation box in the gas phase and allowed to condense at the free surface of a growing film. The just-deposited molecules are maintained at an elevated temperature to mimic the effect of enhanced surface mobility; these molecules are then gradually cooled to the substrate temperature. After an energy minimization step, the next

group of molecules is introduced. The process is continued until a vapor-deposited film with a thickness of roughly 15 molecular diameters is obtained. These simulations were performed over a range of substrate temperatures. Fig. 4 shows that the molecular orientation in these simulated vapor-deposited films has the same dependence upon substrate temperature as observed in the experiments shown in Fig. 3*A*. In particular, near T_g, the simulated glasses display a weak tendency to orient molecules normal to the substrate, and at lower temperatures a stronger tendency to orient molecules in the plane of the substrate. The simulated glasses exhibit high density and high onset temperatures, in analogy to Fig. 2 (*SI Text*, *Simulations*). Note that this model was designed to explore the generic features of the experiments and has not been parameterized against atomistic simulations, ab initio calculations, or the experimental results.

Molecular orientation in vapor-deposited glasses can be understood to be a remnant of the molecular orientation present near the surface of the equilibrium liquid. We performed additional simulations, using conventional molecular dynamics, to investigate the order parameter and density for thin films of the equilibrium liquid above T_g; these results are shown in Fig. 5 *A* and *B*. Molecules nearest the free surface ($0 < z < 1.5$, in bead diameter units) have a propensity to lie in the plane of the surface. Further from the surface as the liquid reaches the bulk density ($1.5 < z < 3.5$), molecules have a tendency to orient vertically, and this tendency becomes stronger at lower temperatures. Beyond $z = 3.5$, orientation in the liquid is isotropic, as expected for a bulk liquid. At a given deposition rate, there will be some substrate temperature at which surface mobility is just sufficient to equilibrate the surface to a depth of $z = 2.5$ but no further. Molecules at this depth show a tendency toward vertical orientation and will become locked into this orientation when further deposition takes place.

Within the context of the simulations of the deposition process, we can test this hypothesis for the origin of molecular orientation in the glass. We quantify the depth at which molecular orientation becomes fixed during deposition by calculating $\langle P_2(\hat{\mu} \cdot \hat{\mu}_{final})\rangle$, where $\hat{\mu}_{final}$ is the orientation of the long axis of the molecule after the deposition is complete. This function, shown in Fig. 5*C*, approaches unity as each molecule attains its final orientation in the glass and we use the 1/e point of this approach to define the thickness of the equilibrated layer at the free surface during deposition. We observe that equilibration to $z \sim 2.5$ occurs near $T_{substrate}/T_g = 0.99$, and Fig. 4 shows that this indeed is the vapor-deposited glass with the maximum value of S_z. At $T_{substrate}/T_g = 0.86$, the surface will only be equilibrated to a depth of $z \sim 1$. At this depth, molecules tend to be oriented parallel to the surface and this orientation becomes locked into the glass. When $T_{substrate}/T_g$ is above 1.02, mobility extends far enough into the film to ensure that an isotropic set of orientations are trapped in the vapor-deposited glass. We note that this explanation accounts for the qualitatively different dependences of S_z and $\Delta\rho$ upon the substrate temperature, as shown in Figs. 2 and 3.

The simulations suggest that orientation in vapor-deposited organic glasses is explained by two factors: (*i*) molecular orientation near the free surface of the equilibrium liquid at $T_{substrate}$, and (*ii*) mobility near the surface of the glass. The first factor might be investigated in greater detail with atomistic simulations and surface sensitive spectroscopy (33), whereas a number of new experimental methods are available to probe dynamics at the surface of glasses (25, 34). Structure at liquid surfaces is an active area of study (35, 36), and our results indicate that physical vapor deposition might be a useful tool in this endeavor.

Discussion

We anticipate that these results can influence work in organic electronics and related fields in several ways. Molecular orientation is already recognized as a key factor influencing device performance (1, 2, 4, 5, 10–15, 37, 38) and our results provide a predictive tool for choosing the deposition temperature needed to produce the desired orientation, effectively adding a dimension to device design. The ability to predictably tune refractive indices across a wide range is analogously useful in applications that rely on redirection of light, such as waveguides or antireflective coatings (39). Although the results shown in Fig. 3 are only known to apply to molecules of roughly linear shape, they suggest that a more general understanding of molecular orientation in vapor-deposited glasses may be attainable with high-throughput characterization and simulations. It is possible that liquid-crystal–forming molecules or systems with specific intermolecular interactions will exhibit orientation trends distinct from those found here, and this would be a further route toward control of molecular anisotropy in glassy solids. High-throughput experiments that directly measure charge mobility (16–18) would complement the results presented here.

Because the three systems investigated here show the density and onset temperatures expected for stable glasses, we anticipate that organic semiconductors will generally have other stable glass properties that should provide control over some known failure modes (40–42). For example, high glass density reduces uptake of atmospheric gases which can cause chemical degradation (43). Also, it is likely that stable semiconducting glasses will transform via a surface-initiated mobility front (26, 44, 45), allowing the

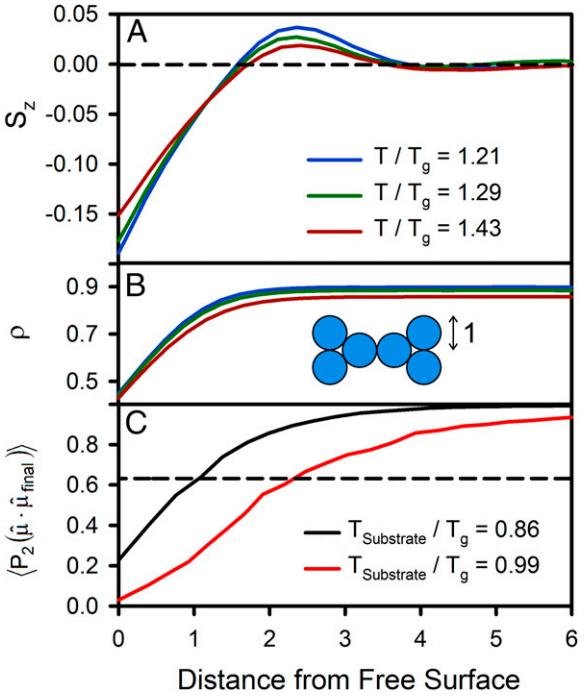

Fig. 5. Simulation results for the equilibrium liquid and the vapor-deposition process reveal the origin of molecular orientation in the glass. (*A*) The order parameter S_z for the equilibrium liquid at three temperatures above T_g. Molecules at the free surface ($z = 0$) tend to lie parallel to the surface. Just below the free surface ($z \sim 2.5$, in units of the bead diameter), molecules adopt a slight vertical orientation, and this tendency becomes stronger as the temperature decreases. (*B*) The number density (ρ) of the equilibrium liquid at three temperatures. The free surface ($z = 0$) is defined as the position where the density drops to half of the bulk value. (*C*) The immobilization of molecular orientation during deposition at two substrate temperatures. The y axis displays a local order parameter defined by the orientation of individual molecules relative to their final orientation. Molecular orientation becomes fixed closer to the free surface at lower substrate temperatures. The data in *A* and *B* were acquired using conventional molecular dynamics to equilibrate the liquid at the simulation temperature and is the average of 5,000 configurations. The x axis of all panels is provided in units of the bead diameter.

possibility of further enhancing thermal stability by engineering device interfaces.

These results also open avenues for increasing our fundamental understanding of glasses. At present, it is hard to discern what features of local packing provide the structural basis for high stability glasses. The anisotropic packing of these organic semiconductors provides additional experimental observables related to local structure [e.g., molecular orientation and anisotropic charge mobility (7)], thus providing the opportunity for a comprehensive understanding of structural stability in amorphous packing. One could ask whether it is possible to prepare stable glasses that do not have substantial anisotropy. Such systems would be ideal for understanding how the Kauzmann entropy crisis is resolved for very deeply supercooled liquids (46). Finally, anisotropy can be viewed as a type of ordering that drives a glass toward crystalline or liquid crystalline states. The existence of highly anisotropic glasses raises the question whether there is a level of anisotropy that cannot be surpassed while maintaining the macroscopic homogeneity associated with amorphous packing.

Materials and Methods

Experimental Methods. Our procedure for preparation and measurement of samples has previously been discussed (21). Physical vapor deposition of samples takes place inside a vacuum chamber with base pressure near 10^{-7} torr. After evacuating the chamber with a turbomolecular pump (occasionally in concert with cryopumping to lower the partial pressure of water) a copper cold cup is cooled via liquid-nitrogen–cooled gas. This copper cup is mechanically coupled to two fingers supporting a single substrate that are independently temperature controlled using a Lakeshore 336 (Lakeshore Cryotronics), resistive heater cartridges (Southwest Heater Corporation), and 100-Ω platinum resistive temperature detectors (Omega). To produce a library of glasses of a single compound, the two fingers are set to different temperatures. After the gradient of temperatures in the substrate is established, it is held constant until the end of the deposition.

TPD and NPB were purchased from Sigma-Aldrich. DSA-Ph, 99% HPLC grade, was purchased from Luminescence Technology Corporation. All compounds were used without further purification. The compound for deposition is placed inside an alumina crucible that is heated by flow of current through resistive wire. The crucible is ∼18 cm away from the substrate. The deposition rate is controlled to be constant using a quartz crystal microbalance, and the true deposition rate is determined by the mean sample thickness divided by the duration of the deposition. The true deposition rate for TPD is 0.24 ± 0.03, NPB is 0.23 ± 0.03, and DSA-Ph is 0.27 ± 0.03, all in nm/s. Substrate temperatures are confirmed by comparison of temperature gradient samples to single-temperature substrates. The glass transition temperature, T_g, for TPD and NPB is determined by heating and cooling at 1 K/min while measuring with spectroscopic ellipsometry. T_g for DSA-Ph is determined by differential scanning calorimetry at 10 K/min.

Once the deposition is complete, the entire sample is brought to 293 K. The vacuum chamber is vented with nitrogen and the samples are either measured immediately or stored at 253 K before measurement. A temperature gradient sample of TPD was measured before and after storage at 253 K for 6 mo with no detectable evolution of its optical constants.

Simulation Methods. The coarse-grained TPD molecule considered here (Fig. 4, *Inset*) consists of six spherical beads representing the aromatic rings of the actual molecule (Fig. 1*E*). Each sphere interacts through a Lennard-Jones (LJ) potential energy function with parameters $\sigma_{bb} = 1.0$, $\varepsilon_{bb} = 1.0$. The cutoff distance for the potential is $r_c = 2.5$ with a smooth decay starting at $r = 2.4$. To maintain the intramolecular structure, the six LJ particles of one molecule are connected by seven stiff bonds ($l_b = 1.0$, $k_b = 1{,}000$). Angle potentials are applied to four groups of three particles that include two interior beads and one of the exterior beads ($\theta = 150°$, $k_{angle} = 1{,}000$). No additional restrictions are applied on the relative rotation of the two halves of the molecule about the longitudinal $(\hat{\mu})$ axis.

The simulation box size is 20 $\sigma_{bb} \times 20$ σ_{bb} in the plane of the substrate $(\hat{x} - \hat{y})$, and at least 10 σ_{bb} larger than the deposited film thickness normal to the substrate $(\hat{z})$. Periodic boundary conditions are applied in the $\hat{x} - \hat{y}$ plane. The substrate is generated from 1,000 randomly placed smaller LJ particles. The LJ potential parameters for the substrate are chosen in such a way as to minimize their effect on deposited molecules and prevent undesirable ordering (47). The parameters for the interaction with other substrate atoms are $\sigma_{ss} = 0.6$, $\varepsilon_{ss} = 0.1$, and with beads representing benzene rings $\sigma_{sb} = 1.0$ and $\varepsilon_{sb} = 1.0$, with a cutoff distance of $2.5\sigma_{\alpha\beta}$, where $\alpha,\beta \in$ s,b. All substrate atoms are fixed to their random initial position with harmonic springs.

The simulated vapor deposition process is analogous to that reported earlier (9, 32). Iterative cycles are repeated until a film with thickness of ∼35 σ_{bb} is grown. Each cycle consists of (*i*) introduction of four randomly oriented molecules in proximity of the film surface, (*ii*) equilibration of newly introduced molecules at high temperature $(T = 1.0)$, (*iii*) linear cooling of these molecules to the substrate temperature in 7×10^5 time steps, and (*iv*) energy minimization of the entire system. The previously deposited molecules and the substrate particles are maintained at a constant temperature throughout the process using a separate thermostat. For the results shown in Fig. 4, the order parameter is calculated from the middle layer of the films to reduce the effect of the substrate and free surface.

The equilibrium liquid profiles in Fig. 5 *A* and *B* were obtained by conventional molecular dynamics simulations and represent time averages over simulation runs comprising 10^8 time steps. All simulations were performed using the Large-Scale Atomic/Molecular Massively Parallel Simulator package (48) in the canonical ensemble with simulation time step of 0.001.

ACKNOWLEDGMENTS. We thank Daisuke Yokoyama and Ken Kearns for helpful discussions. The experimental work was supported by the US Department of Energy, Office of Basic Energy Sciences, Division of Materials Sciences and Engineering, Award DE-SC0002161 (to S.S.D., D.M.W., and M.D.E.). The simulations were supported by National Science Foundation DMR-1234320 (to I.L. and J.J.d.P.).

1. Yokoyama D, Setoguchi Y, Sakaguchi A, Suzuki M, Adachi C (2010) Orientation control of linear-shaped molecules in vacuum-deposited organic amorphous films and its effect on carrier mobilities. *Adv Funct Mater* 20(3):386–391.
2. Frischeisen J, Yokoyama D, Endo A, Adachi C, Brütting W (2011) Increased light outcoupling efficiency in dye-doped small molecule organic light-emitting diodes with horizontally oriented emitters. *Org Electron* 12(5):809–817.
3. Yokoyama D (2011) Molecular orientation in small-molecule organic light-emitting diodes. *J Mater Chem* 21(48):19187–19202.
4. Oh-e M, Ogata H, Fujita Y, Koden M (2013) Anisotropy in amorphous films of cross-shaped molecules with an accompanying effect on carrier mobility: Ellipsometric and sum-frequency vibrational spectroscopic studies. *Appl Phys Lett* 102(10):101905.
5. Tumbleston JR, et al. (2014) The influence of molecular orientation on organic bulk heterojunction solar cells. *Nat Photonics* 8(5):385–391.
6. Marchetti AP, Haskins TL, Young RH, Rothberg LJ (2014) Permanent polarization and charge distribution in organic light-emitting diodes (OLEDs): Insights from near-infrared charge-modulation spectroscopy of an operating OLED. *J Appl Phys* 115(11):114506.
7. Wakamiya A, et al. (2014) On-top π-stacking of quasiplanar molecules in hole-transporting materials: Inducing anisotropic carrier mobility in amorphous films. *Angew Chem Int Ed Engl* 53(23):5800–5804.
8. Lin HW, et al. (2004) Anisotropic optical properties and molecular orientation in vacuum-deposited ter(9,9-diarylfluorene)s thin films using spectroscopic ellipsometry. *J Appl Phys* 95(3):881–886.
9. Lin P-H, Lyubimov I, Yu L, Ediger MD, de Pablo JJ (2014) Molecular modeling of vapor-deposited polymer glasses. *J Chem Phys* 140(20):204504.
10. Mayr C, Taneda M, Adachi C, Brütting W (2014) Different orientation of the transition dipole moments of two similar Pt(II) complexes and their potential for high efficiency organic light-emitting diodes. *Org Electron* 15(11):3031–3037.
11. Komino T, Tanaka H, Adachi C (2014) Selectively controlled orientational order in linear-shaped thermally activated delayed fluorescent dopants. *Chem Mater* 26(12):3665–3671.
12. Kuma H, Hosokawa C (2014) Blue fluorescent OLED materials and their application for high-performance devices. *Sci Technol Adv Mater* 15(3):034201.
13. Ogiwara T, et al. (2014) Efficiency improvement of fluorescent blue device by molecular orientation of blue dopant. *J Soc Inf Disp* 22(1):76–82.
14. Kim B, et al. (2013) Synthesis and elecpagetroluminescence properties of highly efficient blue fluorescence emitters using dual core chromophores. *J Mater Chem C* 1(3): 432–440.
15. Kearns KL, et al. (2014) *SPIE Organic Photonics + Electronics*, eds So F, Adachi C (International Society for Optics and Photonics, Bellingham, WA), Vol 9183, p 91830F.
16. Yokoyama D, Sasabe H, Furukawa Y, Adachi C, Kido J (2011) Molecular stacking induced by intermolecular C–H···N hydrogen bonds leading to high carrier mobility in vacuum-deposited organic films. *Adv Funct Mater* 21(8):1375–1382.
17. Chen W-C, et al. (2014) Staggered face-to-face molecular stacking as a strategy for designing deep-blue electroluminescent materials with high carrier mobility. *Adv Opt Mater* 2(7):626–631.
18. Hiszpanski AM, Loo Y-L (2014) Directing the film structure of organic semiconductors via post-deposition processing for transistor and solar cell applications. *Energy Environ Sci* 7(2):592–608.
19. Kim C, Marshall KL, Wallace JU, Chen SH (2008) Photochromic glassy liquid crystals comprising mesogenic pendants to dithienylethene cores. *J Mater Chem* 18(46):5592–5598.

20. Swallen SF, et al. (2007) Organic glasses with exceptional thermodynamic and kinetic stability. *Science* 315(5810):353–356.
21. Dalal SS, Fakhraai Z, Ediger MD (2013) High-throughput ellipsometric characterization of vapor-deposited indomethacin glasses. *J Phys Chem B* 117(49):15415–15425.
22. Leon-Gutierrez E, Garcia G, Lopeandia AF, Clavaguera-Mora MT, Rodríguez-Viejo J (2010) Size effects and extraordinary stability of ultrathin vapor deposited glassy films of toluene. *J Phys Chem Lett* 1(1):341–345.
23. Leon-Gutierrez E, Sepúlveda A, Garcia G, Clavaguera-Mora MT, Rodríguez-Viejo J (2010) Stability of thin film glasses of toluene and ethylbenzene formed by vapor deposition: An in situ nanocalorimetric study. *Phys Chem Chem Phys* 12(44): 14693–14698.
24. Ahrenberg M, et al. (2013) In situ investigation of vapor-deposited glasses of toluene and ethylbenzene via alternating current chip-nanocalorimetry. *J Chem Phys* 138(2): 024501.
25. Zhu L, et al. (2011) Surface self-diffusion of an organic glass. *Phys Rev Lett* 106(25): 256103.
26. Léonard S, Harrowell P (2010) Macroscopic facilitation of glassy relaxation kinetics: Ultrastable glass films with frontlike thermal response. *J Chem Phys* 133(24):244502.
27. Brian CW, Yu L (2013) Surface self-diffusion of organic glasses. *J Phys Chem A* 117(50): 13303–13309.
28. Dawson KJ, Zhu L, Yu L, Ediger MD (2011) Anisotropic structure and transformation kinetics of vapor-deposited indomethacin glasses. *J Phys Chem B* 115(3):455–463.
29. Singh S, de Pablo JJ (2011) A molecular view of vapor deposited glasses. *J Chem Phys* 134(19):194903.
30. Yokoyama D, Sakaguchi A, Suzuki M, Adachi C (2008) Horizontal molecular orientation in vacuum-deposited organic amorphous films of hole and electron transport materials. *Appl Phys Lett* 93(17):173302.
31. Yokoyama D, Sakaguchi A, Suzuki M, Adachi C (2009) Horizontal orientation of linear-shaped organic molecules having bulky substituents in neat and doped vacuum-deposited amorphous films. *Org Electron* 10(1):127–137.
32. Lyubimov I, Ediger MD, de Pablo JJ (2013) Model vapor-deposited glasses: Growth front and composition effects. *J Chem Phys* 139(14):144505.
33. Hommel EL, Allen HC (2003) 1-methyl naphthalene reorientation at the air–liquid interface upon water saturation studied by vibrational broad bandwidth sum frequency generation spectroscopy. *J Phys Chem B* 107(39):10823–10828.
34. Chai Y, et al. (2014) A direct quantitative measure of surface mobility in a glassy polymer. *Science* 343(6174):994–999.
35. Waring C, Bagot PAJ, Costen ML, McKendrick KG (2011) Reactive scattering as a chemically specific analytical probe of liquid surfaces. *J Phys Chem Lett* 2(1):12–18.
36. Andersson G, Ridings C (2014) Ion scattering studies of molecular structure at liquid surfaces with applications in industrial and biological systems. *Chem Rev* 114(17): 8361–8387.
37. Lee SS, Loo Y-L (2010) Structural complexities in the active layers of organic electronics. *Annu Rev Chem Biomol Eng* 1(1):59–78.
38. Noguchi Y, et al. (2013) Influence of the direction of spontaneous orientation polarization on the charge injection properties of organic light-emitting diodes. *Appl Phys Lett* 102(20):203306.
39. Yokoyama D, Nakayama K, Otani T, Kido J (2012) Wide-range refractive index control of organic semiconductor films toward advanced optical design of organic optoelectronic devices. *Adv Mater* 24(47):6368–6373.
40. Jørgensen M, Norrman K, Krebs FC (2008) Stability/degradation of polymer solar cells. *Sol Energy Mater Sol Cells* 92(7):686–714.
41. Krebs FC, Norrman K (2007) Analysis of the failure mechanism for a stable organic photovoltaic during 10 000 h of testing. *Prog Photovolt Res Appl* 15(8):697–712.
42. Grossiord N, Kroon JM, Andriessen R, Blom PWM (2012) Degradation mechanisms in organic photovoltaic devices. *Org Electron* 13(3):432–456.
43. Dawson KJ, Kearns KL, Ediger MD, Sacchetti MJ, Zografi GD (2009) Highly stable indomethacin glasses resist uptake of water vapor. *J Phys Chem B* 113(8):2422–2427.
44. Sepúlveda A, Leon-Gutierrez E, Gonzalez-Silveira M, Clavaguera-Mora MT, Rodríguez-Viejo J (2012) Anomalous transformation of vapor-deposited highly stable glasses of toluene into mixed glassy states by annealing above Tg. *J Phys Chem Lett* 3(7): 919–923.
45. Wolynes PG (2009) Spatiotemporal structures in aging and rejuvenating glasses. *Proc Natl Acad Sci USA* 106(5):1353–1358.
46. Kauzmann W (1948) The nature of the glassy state and the behavior of liquids at low temperatures. *Chem Rev* 43(2):219–256.
47. Haji-Akbari A, Debenedetti PG (2014) The effect of substrate on thermodynamic and kinetic anisotropies in atomic thin films. *J Chem Phys* 141:024506.
48. Plimpton S (1995) Fast parallel algorithms for short-range molecular dynamics. *J Comput Phys* 117(1):1–19.
49. Woollam JA, et al. (1999) Overview of variable angle spectroscopic ellipsometry (VASE), Part I: Basic theory of typical applications. *SPIE Proc* CR72:3–28.
50. Dalal SS, Ediger MD (2012) Molecular orientation in stable glasses of indomethacin. *J Phys Chem Lett* 3:1229–1233.
51. Vuks MF (1966) Determination of the optical anisotropy of aromatic molecules from the double refraction of crystals. *Opt Spectrosc* 20:361–364.
52. Vuks MF (1966) On the theory of double refraction of liquids and solution in an electric field. *Opt Spectrosc* 21:383–388.